A Weighted Contrast Enhancement Autofocus Algorithm

Le-tian Zeng, Yi Liang, Hong-xian Wang, Meng-dao Xing
National Laboratory of Radar Signal Processing
Xidian University
Xi'an, China
zengletian2@163.com

***Abstract*—Motion errors are inevitably introduced when data are acquired and considerably degrade the image quality in terms of geometric resolution, radiometric accuracy and image contrast, especially in high resolution spotlight synthetic aperture radar (SAR) imagery. In this paper, we describe a weighted contrast enhancement autofocus algorithm that is based on spatially variant model and adopts a mean square error (MSE) phase estimator in which the weights are determined by their contrasts of corresponding sub-scenes. The presented algorithm is very robust to deal with substantial errors over a variety of scenes even in conditions of homogenous areas with no prominent point scatters and enables the utilization of fast Fourier transform (FFT). Experimental results obtained by the proposed methods confirm that the analysis extends well to realistic situations.**

***Index Terms*—Synthetic Aperture Radar (SAR), Spatially Variant Errors, Weighted Contrast Enhancement**

I. INTRODUCTION

In modern synthetic aperture radar (SAR) applications, data-driven methods are indispensably developed to estimate and compensate for the residual phase errors beyond the capacity of the navigation systems so that a well-focused image can be obtained. However, the phase errors are essentially spatial-variant, which may deteriorate the SAR focus [1] in the range dimension with many range bins if not compensated.

There are a number of data-driven autofocus techniques that attempt to correct motion errors [2, 3]. The conventional map-drift (MD) autofocus algorithm [4] is to model the motion error as a second-order polynomial and estimates the Doppler Rate of the radar echo so as to calculate the corresponding acceleration, but it is inadequate in high resolution SAR imaging with a long synthetic aperture as well as an unpredictable trajectory. As the industry standard, phase gradient autofocus (PGA) [5] is a nonparameterized method which computes the first derivative of the phase error based on the information about isolated point scatters. However, poor results are obtained when it comes to the content with low contrast and low signal-to-noise ratio (SNR) or homogeneous areas in the image, such as desert, grassland and sea surface. A more recent class encompasses algorithms that determine the phase error estimate which minimizes or maximizes a particular cost function [6, 7] and correct the blurred images. Nevertheless, this image restoration technique is computationally intensive and usually liable to be influenced by its specific iterative strategy in certain circumstances.

In this paper, we describe a weighted contrast enhancement autofocus algorithm that is based on spatially variant model and adopts a mean square error (MSE) phase estimator in which the weights are determined by their contrasts of corresponding sub-scenes. Our algorithm not only improves the estimation accuracy, but also is very robust to deal with substantial errors over a variety of scenes even in conditions of no prominent point scatters. Actual SAR data using the proposed methods confirm that the analysis extends well to realistic situations.

II. MOTION ERROR MODEL

Assume the SAR platform flies with a constant velocity at the height of H with no deviations following $y = z = 0$, as shown as Fig.1. However, in actual cases, the deviation from the nominal path in the y and z direction are $\left[\Delta y(0), \Delta y(1), ..., \Delta y(N-1)\right]$ and $\left[\Delta z(0), \Delta z(1), ..., \Delta z(N-1)\right]$ in the listed order, where N represents the number of echoes. So the estimated phase error $\Delta\varphi_i(n)$ in the i th range cell can be written as

$$\Delta\varphi_i(n) = \frac{4\pi}{\lambda}\Delta R_i(n) \approx \frac{4\pi}{\lambda}\left(\Delta y(n)\cdot\sin\alpha_i + \Delta z(n)\cdot\cos\alpha_i\right) \quad (1)$$

where $\Delta R_i(n)$ is the slant range error related to the i th range

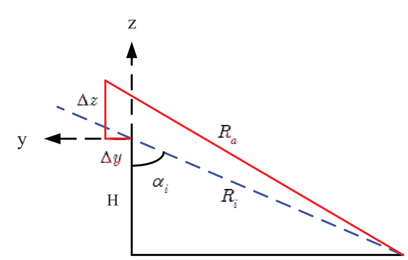

Fig.1. Phase error correction model

cell, $i=1,2,\cdots,M$ describes the index of the samples within each echo and α_i represents the incident angle of i th range bin. Considering the spatially variance of the phase error and rewriting Equation 1 via the vector notations, we have

$$\begin{bmatrix} \Delta\Phi(1,:) \\ \Delta\Phi(2,:) \\ \vdots \\ \Delta\Phi(M,:) \end{bmatrix} = \frac{4\pi}{\lambda} \begin{bmatrix} \sin\alpha_1 & \cos\alpha_1 \\ \sin\alpha_2 & \cos\alpha_2 \\ \vdots & \vdots \\ \sin\alpha_M & \cos\alpha_M \end{bmatrix} \begin{bmatrix} \Delta y(1) & \cdots & \Delta y(N) \\ \Delta z(1) & \cdots & \Delta z(N) \end{bmatrix} \quad (2)$$

where $\Delta\Phi(i,:)=\left[\Delta\varphi_i(1) \quad \Delta\varphi_i(2) \quad \cdots \quad \Delta\varphi_i(N)\right]$ denotes the azimuthal phase error in the i th range resolution cell. However, the true range error of the i th range resolution cell equals the actual range minus the nominal value of the distance R_i between this range bin and the ideal flight trajectory, so the corresponding phase error can be represented as

$$\Delta\varphi_i^r(n)=\frac{4\pi}{\lambda}\left(R_a(n)-R_i\right) \quad (3)$$

wher $R_a(n)=\sqrt{\left(\sqrt{R_i^2-H^2}+\Delta y(n)\right)^2+\left(H+\Delta z(n)\right)^2}$ defines the actual range from the platform to the i th range resolution cell at azimuth position n. And the true phase error matrix are given by

$$\begin{bmatrix} \Delta\Phi^r(1,:) \\ \Delta\Phi^r(2,:) \\ \vdots \\ \Delta\Phi^r(M,:) \end{bmatrix} = \frac{4\pi}{\lambda} \begin{bmatrix} R_a(1)-R_1 & \cdots & R_a(N)-R_1 \\ R_a(1)-R_2 & \cdots & R_a(N)-R_2 \\ \vdots & \ddots & \vdots \\ R_a(1)-R_M & \cdots & R_a(N)-R_M \end{bmatrix} \quad (4)$$

In order to take the effects of the spatial variance of the phase error into account, we adopt a weighted scheme to estimate the range-dependent phase error, which will be discussed later.

III. MAXIMUM CONTRAST ALGORITHM

Autofocus usually begins with the range-compressed phase history domain, in which the data are compressed in range but not compressed in azimuth. Suppose the formation of a complex SAR is $f(i,n)$, which is denoted by

$$f(i,n)=\frac{1}{N}\sum_{k=0}^{N-1}u(i,k)\exp(j\frac{2\pi nk}{N}) \quad (5)$$

where $u(i,k)$ represents the azimuth phase history data after range alignment. The indexes $i=0,1,...,M-1$, $k=0,1,...,N-1$ and $n=0,1,...,N-1$ refer to range, aperture positions and azimuth positions in the focused image, separately.

Let us construct a model associated with phase error corrupted data as

$$u(i,k)=u_0(i,k)\exp(j\phi_c(k)) \quad (6)$$

where $u(i,k)$ presents the corrected phase history data and $\phi_c(k)$ is the phase compensation component that cancels out the residual phase error presents in $u_0(i,k)$.

In addition, we define the contrast of a SAR image as

$$C=\frac{1}{M}\sum_{i=0}^{M-1}\frac{\sigma_i}{\mu_i} \quad (7)$$

where $\mu_i=\frac{1}{N}\sum_{n=0}^{N-1}\left|f(i,n)\right|$ and $\sigma_i=\sqrt{\frac{1}{N}\sum_{n=0}^{N-1}(\left|f(i,n)\right|-\mu_i)^2}$ [7]. The contrast takes no statistic information of the isolated scatters into account and does not require the presence of bright point targets. A high contrast measure is indicative of a sharp image, whereas a low contrast signifies that the image is out of focus.

The aim of the autofocus algorithm is to determine and apply the phase correction vector $\phi_c=\left[\phi_c(0),\phi_c(1),...,\phi_c(N-1)\right]$ imposed on the phase history data suggested to maximize the chosen metric C. Since there is no closed-form solution for ϕ_c that maximizes C in Equation 7，we find that an efficient and powerful way for solving this problem is to use conjugate gradient algorithm, which works well in solving a large scale nonlinear optimization and conserves memory. The search, which is based on the gradient-based and iterative-based optimization algorithm, finds coordinates of the maximum contrast measure. The estimate of the phase error deviating from the true kinematic parameters yields blurred images, while good estimates produce focused images. Using this method requires the explicit formulas for the gradient of the contrast function C with respect to the phase correction vector $\phi_c(k)$, which can be shown as [7]

$$\frac{dC}{d\phi_c(k)}=\sum_{i=0}^{M-1}\gamma_i\,\mathrm{Im}\left[u^*(i,k)q(k)\right] \quad (8)$$

where $\gamma_{vi}=\frac{-1}{MN}(\frac{1}{\sigma_i}+\frac{\sigma_i}{\mu_i})$ and $q(k)=\sum_{n=0}^{N-1}\frac{f(i,n)}{\left|f(i,n)\right|}\exp(-j2\pi\frac{nk}{N})$. For the sake of substantially reducing the computational burden for the phase error, a subset with high contrast of the available data is chosen to reconstruct a SAR image while maintains the results of expected quality at the same time.

IV. WEIGHTED CONTRAST ENHANCEMENT ALGORITHM

In this part, we adopt a weighted mean square error (WMSE) phase estimator in which the weights are determined by the contrasts of corresponding sub-blocks. This phase estimation is more robust than phase adjustment by contrast enhancement [7] because it does account for range varying behavior of the phase error while improves the accuracy of the estimate values by adjusting the weights of different range resolution cell data.

In order to perform the described estimation, we establish a weighted mean square error estimator as

$$WMSE(\Delta y(n),\Delta z(n))=\sum_{i=1}^{M}w_i\left(\Delta\Phi(\mathrm{i},n)-\Delta\Phi^r(\mathrm{i},n)\right)^2 \quad (9)$$

where w_i ($i=0,1,...,\mathrm{M}-1$) are the coefficients determined by the contrast of the i th range bin data and can be expressed as $w_i = C_i \Big/ \sum_{i=0}^{M-1} C_i$. Since the range bins with high contrast tend to have more features sensitive to variations in the phase error, the purpose of this optional weight w_i is to put more emphasis on the contribution of high contrast scenes than on that of the low ones to the estimation process of the induced phase error. Therefore, the weighting improves the overall accuracy of the estimation process. By exploiting the WMSE estimator, we have

$$\begin{aligned} &\frac{4\pi}{\lambda}\Delta y(n)\sum_{i=0}^{M-1} w_i \left(\sin\alpha_i\right)^2 + \frac{4\pi}{\lambda}\Delta z(n)\sum_{i=0}^{M-1} w_i \sin\alpha_i \cos\alpha_i \\ &= \sum_{i=0}^{M-1} w_i \Phi^r\left(i,n\right)\sin\alpha_i \end{aligned} \tag{10}$$

$$\begin{aligned} &\frac{4\pi}{\lambda}\Delta y(n)\sum_{i=0}^{M-1} w_i \sin\alpha_i \cos\alpha_i + \frac{4\pi}{\lambda}\Delta z(n)\sum_{i=0}^{M-1} w_i \left(\cos\alpha_i\right)^2 \\ &= \sum_{i=0}^{M-1} w_i \Phi^r\left(i,n\right)\cos\alpha_i \end{aligned} \tag{11}$$

The solution to the Equation 10 and Equation 11 gives the expressions of the trajectory deviation $\Delta y(n)$ and $\Delta z(n)$. However, using the data of a single range bin to estimate the phase error is not liable or robust in practical applications, in which clutters and noises may have a deadly effect on the estimation. Moreover, this method results in an intensive computational burden at the same time. The division of the data set into narrow range sub-swaths can effectively solve this problem and is carried out in the phase history domain where the data are range compressed and azimuth defocused.

First, we break a large data set into V smaller sub-blocks in the range dimension with $M_1 = M/V$ range resolution cells in each sub-block so that the phase error present on the subset data is approximately invariant. Then, space-invariant autofocus operation, in this paper that is maximum contrast algorithm, devotes to averaging over many range bins to improve algorithm performance in terms of error estimation accuracy, instead of utilizing a single range cell data which is liable to be affected by strong clutters and noises. Here, we suppose the distance $R(v)$ （$v = 0,1,...,V-1$）from the SAR ideal trajectory to the center of the v th range sub-block is considered to be the reference range in the spatially variant phase correction procedure. Hence, the range error of the v th range sub-block is calculated and the analogous procedure moves to the next range sub-block. Finally, the phase errors are compensated by the Equation 10 and Equation 11 in SAR data for super results. In order to further reduce the computational burden, we can select part of the range bins in each sub-block to estimate the phase errors within it.

V. Real Data Experiment

In this part, a real data experiment of homogeneous area is conducted to demonstrate the validity of the proposed autofocus algorithm.

In this experiment, the SAR system works in X-band with 0.3m resolution of the focused image in both the range and the azimuth dimensions. The velocity of the platform is about 120m/s with the pulse repeat frequency (PRF) 1250Hz and the sampling rate 800MHz in the range dimension. The height of the carrier is about 6.8km and the reference slant range is 40.8 km. The accuracy of the navigational system is poor. What's more, the imaging scenario mainly consists of farmlands, grasslands and trees without strong scatters, which can be seen as homogeneous areas.

The final images are shown in Fig.2 generated with different methods. For comparison, the SAR images constructed by WLS PGA [8] and the weighted scheme are illustrated in Fig.2 (a) and Fig. 2 (b). One can observe that the results in Fig.2 (a) are inferior to the well-focused SAR image in Fig.2 (b) obtained with the proposed approach, which means residual errors have been reduced to a less amount by the presented approach. The proposed autofocus algorithm is robust, because it does not require strong scatters and can be applied to most scene contents. The entropies of the images in Fig.2 (a) and Fig.2 (b) are 15.94 and 15.80 in the listed order while the contrasts are 0.65 and 0.71, severally. We can see a better focused region in Fig.2 (b) as well as more clear texture about farmlands, crops and grasslands in the imaged area, which certifies the necessity of the weighted scheme to compensate for the spatially variant phase errors and the better performance of the developed autofocus algorithm. This is true not only because the weighted scheme provides superior results, but also because the improvement is more pronounced. Furthermore, the time consumed by removing the spatially variant phase errors in Fig.2 (a) and Fig.2 (b) are respectively 130.86 seconds and 169.14 seconds, which demonstrates the described approach can almost emulate WLS PGA in required time but with better focusing performance. Therefore, the provided example demonstrates the advantages of the proposed algorithm, its capacity to accurately handle range-dependent phase errors in homogeneous scenarios.

Acknowledgment

The authors would like to thank the anonymous reviewers for their valuable comments to improve the quality of study. This work was supported in part by the National Nature Science Foundation of China under grant 61301293, and by the Fundamental Research Funds for the Central Universities under Grant K5051302046.

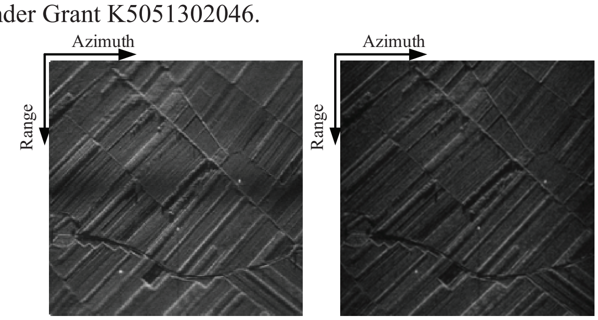

Fig.2 Processed SAR images (a) With WLS PGA (b) With the proposed algorithm

REFERENCES

[1] Y. K. Li, C. Liu, Y. F. Wang, and Q. Wang, "A robust motion error estimation method based on raw data," *IEEE Trans. Geosci. Remote Sens.*, vol. 50, no. 7, pp.2780–2790, July 2012.

[2] G. Xu, M. D. Xing, L. Zhang, and Z. Bao, "Robust autofocusing approach for highly squinted SAR imagery using the extended wavenumber algorithm," *IEEE Trans. Geosci. Remote Sens.*, vol. 51, no.10, pp. 5031-5046, Oct. 2013.

[3] L. Zhang, J. L. Sheng, M. D. Xing, Z.J. Qiao, T. Xiong, and Z. Bao, "Wavenumber-domain autofocus for highly squinted UAV SAR Imagery," *IEEE Trans. Geosci. Remote Sens.*, vol. 12, no. 5, pp.1574–1588, May 2012.

[4] O. O. Bezvesilniy, I. M. Gorovyi, and D. M. Vavriv, "Estimation of phase errors in SAR data by local-quadratic map-drift autofocus," 19th International Radar Symposium, pp. 376-381, 2012.

[5] D. E. Wahl, P. H. Eichel, D. C. Ghiglia, and C. V. Jakowatz, "Phase gradient autofocus - a robust tool for high resolution phase correction," *IEEE Trans. Aerosp. Electron. Syst.*, vol. 30, no. 3, pp. 827-835, July 1994.

[6] R. L. Morrison, M. N. Do, and D. C. Munson, "SAR image autofocus by sharpness optimization: a theoretical study," *IEEE Trans. Image Process*, vol. 16, no. 9, pp. 2309-2321, Sep. 2007.

[7] J. Kolman, Image reconstruction and restoration using constrained optimization algorithms[D]. Dissertation for the Degree of Doctor of Philosophy, West Lafayette, Indiana, Purdue University, 1996.

[8] W. Ye, T. S. Yeo, and Z. Bao, "Weighted least-squares estimation of phase errors for SAR/ISAR autofocus," *IEEE Trans. Geosci. Remote Sens.*, vol. 37, no. 5, pp. 2487-2494, Sep. 1999.